Comparison of two- and four-pole rotors for a high speed bearingless drive

Hubert Mitterhofer*, Wolfgang Amrhein
Institute for Electrical Drives and Power Electronics
Johannes Kepler University
Shareholder of the ACCM GmbH
Linz, Austria

Herbert Grabner
Linz Center of Mechatronics
Shareholder of the ACCM GmbH
Linz, Austria

Abstract

Bearingless drives have found their way into several industrial applications such as pumps, fans and chemical process chambers. In contrast to these drives which run at speeds below 15.000rpm, the suitability of bearingless drives for high speed has first been demonstrated with a bearingless disk drive running up to 115.000rpm in previous works by the authors. This drive uses a permanent magnet rotor with a pole number of two in order to constrain iron losses and generate the highest rotor speed with a certain electrical frequency. Other design criteria such as the rotordynamic behaviour, the radial bearing force or the torque capacity, however, might benefit from a higher pole number. Therefore, this paper will present the comparison of a two-pole and a four-pole rotor for the use in a high speed bearingless drive.

1 Original System

The design under consideration has been presented in [1], therefore, only the key features shall be mentioned here. The flat disk drive as shown in the 3D model on the left side of Fig. 1 uses the magnetic reluctance forces to passively stabilize the rotor in axial and tilt direction. As shown in the scheme on the right side of this figure, only the radial degrees of freedom as well as the torque need to be controlled actively. The drive implements one of the most compact design topologies, since there is only one winding system used for both, torque and bearing force creation. Additionally, the bearingless unit represents the only bearing point in this drive, no other support points are needed.

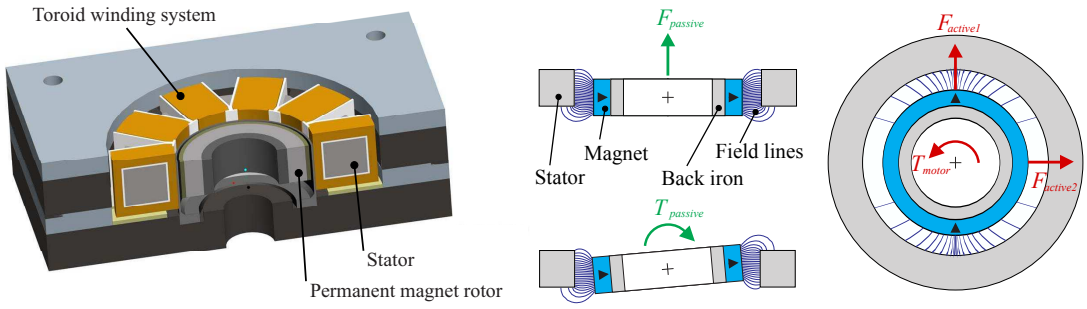

Figure 1: 3D model of the original 2-pole system with passive and active stabilization principle of a bearingless disk drive in general

*hubert.mitterhofer@jku.at, Johannes Kepler University, Altenbergerstrasse 69, 4040 Linz, Austria

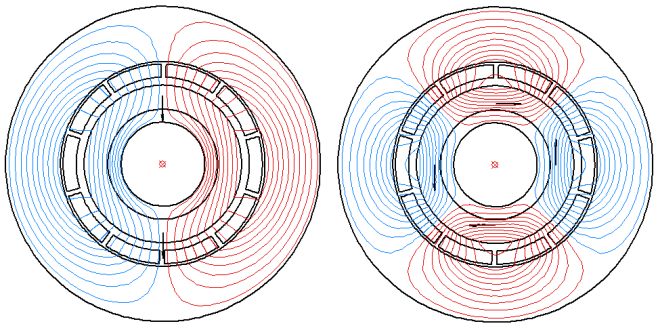

Figure 2: Flux lines for two- and four-pole rotor magnet

Figure 3: Rotor failure due to centrifugal forces at high speeds

2 Geometric Design

In order to retain the sinusoidal air gap flux distribution caused by the diametrically magnetized 2-pole rotor, the compared 4-pole rotor disposes of an ideal Halbach magnetization. The resulting field lines are shown in principle in Fig.2.

Increasing the rotor pole number p shortens the length of the flux path. Therefore, the maximum occurring flux density in the iron is lowered and the stator yoke width can be reduced. In most common optimizations, the fixed geometric dimension is the outer stator diameter d_{so}, since this is usually the most critical dimension for mounting the drive in a certain application. In this case, the outer rotor diameter d_{ro} needs to be retained at the original value. The reason for this lies in the fact that, up to now, the maximum rotational speed is limited by the mechanical strength of the rotor. At a certain speed, the centrifugal forces can no longer be supported by the brittle permanent magnet and the rotor breaks as shown in Fig.3. The additionally available space due to the stator yoke width reduction can, therefore, either be used to decrease d_{so} or to allow more winding space at a constant outer stator diameter. Of course, this entails a changed magnetic air gap due to the slotless stator design which, in turn, influences the passive stiffness. The dependency of the different stiffness components and the system behaviour shall be illuminated below.

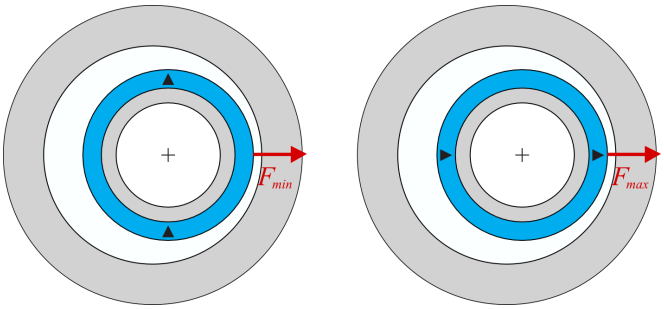

Figure 4: Anisotropic stiffness for the 2-pole rotor

2.1 Radial Stiffness

Moving the permanent magnet rotor out of the ideal stator center causes destabilizing radial forces

$$\mathbf{F} = \begin{bmatrix} F_{rx} \\ F_{ry} \end{bmatrix}. \tag{1}$$

The force per deflection distance is referred to as the radial stiffness c_r in analogy to a mechanical spring. This stiffness varies strongly with the air gap diameter, the axial length, the air gap flux density and also, the pole number.

2-Pole Rotor

Unlike in passive magnetic bearings where usually axially magnetized permanent magnets are used, the radial stiffness is angle dependent in a bearingless drive using a 2-pole rotor. As shown in Fig.4, a rotor movement in direction of the magnetization axis provokes the maximum destabilizing radial force, the minimum value is produced when it is being moved perpendicular to this axis. A mean stiffness value

$$c_{rm,p2} = \frac{c_{r,max} + c_{r,min}}{2} \tag{2}$$

and a variation ratio

$$c_{rx} = \frac{c_{r,max}}{c_{rm,p2}} - 1 \tag{3}$$

can be defined. The forces due to the passive stiffness can be written as

$${}_r\mathbf{F}_c = {}_r\mathbf{C} \cdot {}_r\,\mathbf{q} = \begin{bmatrix} c_{rm,p2}(1+c_{rx}) & 0 \\ 0 & c_{rm,p2}(1-c_{rx}) \end{bmatrix} \begin{bmatrix} {}_rx \\ {}_ry \end{bmatrix} \tag{4}$$

with ${}_r\mathbf{q}$ being the vector of radial rotor deflections (${}_rx$ defines the deflection in the direction of magnetization) and ${}_r\mathbf{C}$ denoting the stiffness matrix. Transforming ${}_r\mathbf{C}$ from the rotor coordinate system to the stationary stator system yields

$${}_s\mathbf{C} = \begin{bmatrix} c_{rm,p2}(1 + c_{rx} \cdot cos(2\varphi(t))) & c_{rm,p2}c_{rx} \cdot sin(2\varphi(t)) \\ c_{rm,p2}c_{rx} \cdot sin(2\varphi(t)) & c_{rm,p2}(1 - c_{rx} \cdot cos(2\varphi(t))) \end{bmatrix}, \tag{5}$$

with $\varphi(t)$ being the rotor angle. As stated above, the radial degrees of freedom are unstable by nature which means that a displacement-proportional controller with its control parameter P fulfilling

$$P > (c_{rm,p2} + c_{rx}) \tag{6}$$

needs to be put in place in order to overcome the destabilizing reluctance effect. As it has been shown in prototype tests presented in [2], this minimum controller requirement is not sufficient in the real life drive. An approximate stiffness ratio of

$$1.8 < \frac{P}{(c_{rm,p2} + c_{rx})} < 2.2 \tag{7}$$

for sub-critical operation, as well as

$$1.5 < \frac{P}{(c_{rm,p2} + c_{rx})} < 1.2 \tag{8}$$

for super-critical operation has been found to be suitable.

4-Pole Rotor

The problem of anisotropic stiffness occurs with a 2-pole rotor only. Given a truly sinusoidal air gap flux distribution and a slotless, i.e. cylindrical, stator core, the stiffness with a higher pole number in the rotor is constant and independent of the direction of deflection according to [3]. In contrast to (5), the stiffness matrix of the 4-pole system

$${}_s\mathbf{C} = \begin{bmatrix} c_{rm,p4} & 0 \\ 0 & c_{rm,p4} \end{bmatrix} \tag{9}$$

is much simpler because there is no angle dependency and no stiffness coupling. Of course, the constant stiffness and, therefore, linear force to displacement relationship is only valid for small deflections.

The fact that the variation term c_{rx} is missing in this case must not mislead to the conclusion, that the stiffness is generally smaller. On the contrary, for a given rotor and stator geometry, the passive radial stiffness is higher with the 4-pole magnet than with the diametrically magnetized one. If the magnet in the original system were to be replaced with a 4-pole magnet of equal material and ring thickness, the constant stiffness $c_{rm,p4}$ would amount to 160% of $c_{rm,p2}$ and to 142% of the peak value $c_{rm,p2}(1+c_{rx})$. Of course, this fact must be taken into account when the optimum stator width is being determined.

2.2 Radial Damping

The mean radial angular resonance frequency is generally defined as

$$\omega_r = \sqrt{\frac{P - c_{rm}}{m_{rotor}}} \tag{10}$$

with m_{rotor} defining the rotor mass. This yields a single value for the 4-pole rotor but results in a whole frequency range of

$$\omega_r\sqrt{1-\varepsilon} < \omega < \omega_r\sqrt{1+\varepsilon} \tag{11}$$

around the resonance frequency becoming unstable for the undamped 2-pole rotor according to [4]. In this equation, ω stands for the angular speed and

$$\varepsilon = \sqrt{\frac{c_{rm,p2}c_{rx}}{P - c_{rm,p2}}} \tag{12}$$

describes the ratio of stiffness anisotropy.

In the present disk drive, there is no inherent damping except for the eddy currents in the winding conductors and the stator back iron. Due to the small amplitude of the radial deflections, their contribution to stabilizing the system is negligible. Therefore, the controller needs to provide sufficient damping. For a chosen coefficient P, the anisotropy ε and, hence, the minimum controller damping value D_{min}, necessary for asymptotically stable rotor operation over the whole frequency range, can be calculated according to [4] as

$$D_{min} = 2m_{rotor}\omega_r\sqrt{0.5(1-\sqrt{1-\varepsilon})}. \tag{13}$$

For the 4-pole rotor, (11) shrinks to the resonance frequency ω_r itself and no minimum damping value needs to be defined. The applied damping value in a real application, however, strongly depends on the tolerable vibrations and surely needs to be considerably larger than the calculated minimum.

2.3 Stabilizing Passive Stiffness

What has been said about isotropic and anisotropic behaviour of the radial stiffness is also true for the tilt stiffness: Tilting of the 2-pole rotor about the axis of magnetization yields the minimum value of tilt stiffness, tilting about the perpendicular axis results in the maximum stiffness. It can be decomposed into a mean value $c_{\alpha m,p2}$ and a variation term $c_{\alpha x}$ which is only relevant for the 2-pole rotor. According to the conducted 3D-FE analysis, the mean value of the 2-pole and the 4-pole rotor coincide.

The axial stiffness does differ if the pole number of the magnet is increased without changing the drive's geometry (-21% for the 4-pole rotor in the original stator design). However, it is evidently not angle dependent in any of the two cases.

3 Iron Losses

One major concern when changing the design of a high speed drive are the possible consequences for the occurring losses. A detailed loss analysis of the present drive has been presented in [5]. The iron losses

$$p_{Fe} = K_h(\frac{f}{f_0})(\frac{B}{B_0})^\beta + K_{ec}(\frac{f}{f_0})^2(\frac{B}{B_0})^\beta \tag{14}$$

were calculated according to Jordan's extension of the classical Steinmetz - model, using three material-specific parameters K_h, K_{ec} and β as well as the field frequency and peak flux density values f_0 and B_0 under which said parameters were obtained. The iron losses turned out to be the most important load-independent loss component. As both the frequency f and the flux density amplitude B of the permanent magnetic field change when using a 4-pole rotor instead of the 2-pole rotor, this part merits closer investigation. The doubled frequency causes higher losses, the reduced flux density in the stator yoke reduces them. For comparing the two situations, the radius-dependent loss density was computed using the pm-field obtained from 2D-FE simulations. After integrating over the stator yoke radius, the two analytical curves shown in Fig.5 have been obtained. Despite the different scaling exponents for frequency and flux density, the losses to be expected are nearly identical for the two cases.

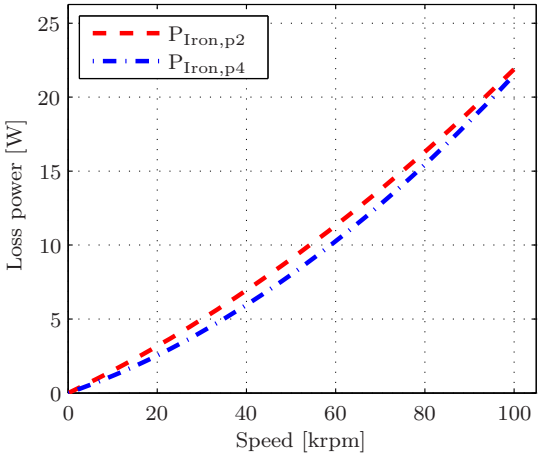

Figure 5: Estimated stator iron loss for the 2-pole and 4-pole rotor

4 Winding

4.1 Requirements

In order to control the three active degrees of freedom independently, a minimum of three phases is necessary. A star connection of the phases reduces power electronic complexity because half bridges can be used instead of full bridges. However, it increases the minimum phase number to four, since in a star connected system, one of the currents cannot be controlled individually. The problem with a symmetrical four phase winding system, however, is that there are four distinct field angles $\varphi = \left\{\frac{\pi}{4}, \frac{3\pi}{4}, \frac{5\pi}{4}, \frac{7\pi}{4}\right\}$ (with $\varphi = 0$ marking the center of one coil) where no four-pole field can be created. In [6], a bearingless disc drive with such a setup of four concentrated coils in combination with a four pole permanent magnet rotor is described. This results in a single phase characteristic of the motor, meaning that at the angles specified above, no torque can be created. In the case of a two-pole permanent magnet rotor, this would mean that at these distinct angles, no radial forces in either x- or y-direction can be created. This is due to the fact that, with p denoting the pole number of the permanent magnetic rotor, a p-pole stator flux will create torque but only a $p \pm 2$-pole stator flux will result in bearing forces [7, ch.16]. As a consequence, only phase numbers of $m = 5$ and $m = 6$ will be considered, since two 3-phase inverters could possibly be used in a real application.

4.2 Winding Scheme

Winding Factor

In order to generate motor torque and bearing forces, the stator field needs to contain a p and a $p \pm 2$ component, respectively. For the case of an interior rotor, the $p + 2$ field is preferable since the Lorentz and the Maxwell forces add up instead of acting in opposing directions as this would be the case for a $p - 2$ field. This can be deduced from the force and torque model presented in [6]. For the two-pole rotor, this is inherently irrelevant. For the four-pole rotor, however, the winding should dispose of a high winding factor for a six-pole field rather than for the two-pole field.

Number of Virtual Slots

Another constraint is the maximum number of virtual slots, i.e. the number of coil sides in the slotless winding. Not only the overall winding complexity but also the total necessary insulation space increases with a rising slot number. Therefore, the number of virtual slots will be limited in order to maintain manufacturability. Of all the possible windings, the only symmetric ones which can be considered dispose of either 10 or 12 slots with either 5 or 6 phases, respectively. The 5-phase winding schemes are exemplarily depicted in Fig.6, the regarded 6-phase schemes are composed alike.

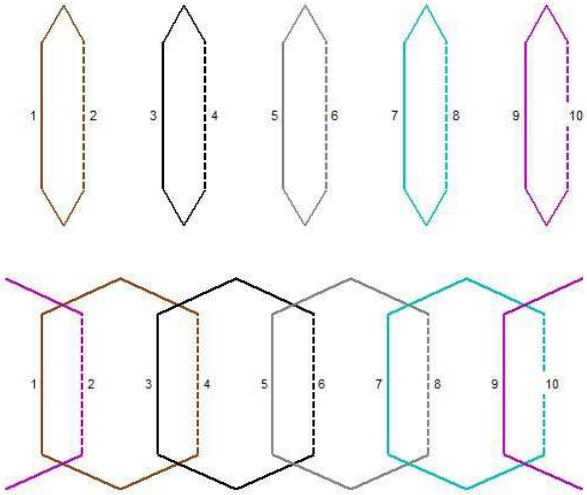

Figure 6: Possible winding schemes with concentrated coils and reduced-pitch coils for 5 phases

4.3 Topology

As mentioned above, the slotless stator form shall be maintained from the initial two-pole design. Maintaining the topology, the resulting winding would be carried out as an air gap winding as shown in the left part of Fig.7. This form is widely used since it is the standard form applied in slotted stators. Especially for a small winding pitch y_n, specifying the number of virtual slot steps from one winding side to the other, the air gap winding is advantageous. For higher y_n, however, the winding heads can become very large.

Another possible winding topology is the toroidal winding form, depicted in the right half of Fig.7. For stator cores with short axial length l_{fe}, small yoke widths b_{sy} and high values of y_n, the required wire length can be reduced significantly. It is, however, essential to remark that the two winding parts need to be wound in opposite direction in order to dispose of the same characteristics and the same current direction in the active winding parts as the air gap winding. This is true under the tacit assumption, that the entire flux is conducted within the iron stator core and no stray flux occurs. This assumption, however, should pose no problem since the stator yoke can be designed to fulfill this very condition.

The decision, which winding form should be used can be taken based upon the manufacturability and the total wire length which, of course, should be minimized. The latter can be

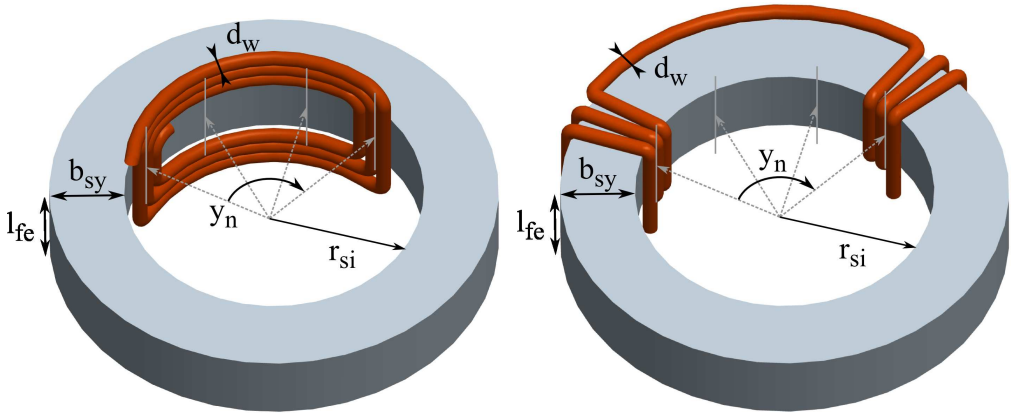

Figure 7: Air gap and toroid winding form with indicated exemplary current directions

	Number of slots / phases / slot steps			
	10/5/1	10/5/3	12/6/1	12/6/3
$l_{cu,toroid}$ (rel.)	95.9%	100%	95.6%	98.9%
$l_{cu,airgap}$ (rel.)	74.6%	136.1%	69.4%	120.7%

Table 1: Wire length for different winding forms and topologies relative to the realized prototype

calculated as

$$l_{cu,airgap} = 2n_w \cdot ((r_{si} + \frac{b_{sy}}{2}) \cdot \frac{2\pi y_n}{n_s} + (l_{fe} + b_{sy}) + d_w) \tag{15}$$

for the air gap winding and as

$$l_{cu,toroid} = 2n_w \cdot (2b_{sy} + 2l_{fe} + 4d_w) + 2r_{si} \cdot \frac{2\pi y_n}{n_s} \tag{16}$$

for the toroid form where d_w, r_{si}, n_w and n_s stand for the wire diameter, the inner stator radius, the number of windings per coil and the total number of slots, respectively. It needs to be remarked, that the radius of the air gap winding head was enlarged by $\frac{b_{sy}}{2}$ in order to provide sufficient space for the emerging winding heads of the coils placed in the slots in between the two winding parts. Of course, this further lengthens the winding heads but is necessary to provide a more realistic comparison. The results are listed in Table 1.

The question of manufacturability is difficult to decide as long as the drive is not designed to fit a certain application. In general, however, the air gap coils need to be self-supporting while the toroid coils can be wound directly onto the isolated stator. This can be a significant advantage if a segmented stator is used.

4.4 Force and Torque Evaluation

In order to estimate the torque and force capacity of the respective winding form, the winding factors for the necessary stator field components are compared in Table 2.

	Number of slots / phases / slot steps			
	10/5/1	10/5/3	12/6/1	12/6/3
Winding factor $p = 2$	0.31	0.81	0.26	0.71
Winding factor $p = 4$	0.59	0.95	0.5	1
Winding factor $p = 6$	0.81	0.31	0.71	0.71

Table 2: Comparison of winding factors

For the 2-pole rotor, the $p + 2$ field gives a clear indication about the possible bearing force capacity. As mentioned above, this cannot be applied directly to the 4-pole rotor since the combination of the $p - 2$ and $p + 2$ field component needs to be considered. Therefore, the coefficients for the torque and force generation capability, k_T and k_F, are also used for evaluation as proposed in [8].

First, the angle dependent matrix $\mathbf{K}_m(\varphi)$ has to be found, defining the relationship between the force and torque vector

$$\mathbf{Q} = \begin{bmatrix} F_{rx}(\varphi) \\ F_{ry}(\varphi) \\ T(\varphi) \end{bmatrix} \tag{17}$$

and the phase currents for the m phases

$$\mathbf{i} = \begin{bmatrix} i_1 \\ \vdots \\ i_m \end{bmatrix} \tag{18}$$

as

$$\mathbf{i} = \mathbf{K}_m(\varphi)\mathbf{Q}. \tag{19}$$

Calculating the currents

$$\mathbf{i}_{Fx} = \mathbf{K}_m(\varphi) \begin{bmatrix} 1 \\ 0 \\ 0 \end{bmatrix} \tag{20}$$

$$\mathbf{i}_{Fy} = \mathbf{K}_m(\varphi) \begin{bmatrix} 0 \\ 1 \\ 0 \end{bmatrix} \tag{21}$$

ensures that in the respective situation only the demanded force component is produced without exciting any other force or torque. Finally, [8] defines the mentioned force and torque constants as

$$k_F = \frac{2m}{\sum_{i=1}^{m}\sum_{j=1}^{2} rms(\mathbf{K}_{m_{i,j}})} \tag{22}$$

and

$$k_T = \frac{2m}{\sum_{i=1}^{m} rms(\mathbf{K}_{m_{i,3}})}, \tag{23}$$

		Number of slots / phases / slot steps			
		10/5/1	10/5/3	12/6/1	12/6/3
2-pole rotor	k_F [mN/A]	272	439	283	565
	k_T [mN m/A]	1.3	5.5	1.1	5.6
	Torque @ 5 A/mm² [mN m]	5.7	23.5	3.7	19.5
4-pole rotor	k_F [mN/A]	91	184	90	230
	k_T [mN m/A]	4.0	7.2	4.0	9.4
	Torque @ 5 A/mm² [mN m]	16.9	30.3	13.6	32.2

Table 3: Comparison of torque and bearing force capabilities

respectively. These constants have been evaluated for the 4 regarded winding schemes for both, 2-pole and 4-pole rotor (Table 3). The torque constant, however, needs to be understood with regard to the drive design. Since the copper surface per phase is smaller in the 6-phase system, the permissible phase current is lower when both the winding number and the current density are constant. Therefore, the total motor torque for a current density of 5 A/mm² is also given in the table. As expected, high torque values can be created using a 4-pole rotor. The possible active bearing forces, however, fall clearly short of the values which can be achieved with the 2-pole rotor.

5 Conclusion

In the above sections, the main effects of a change in the rotor pole number of a bearingless disk drive have been described. The main conclusions drawn from this analysis are the following:

- The stator yoke width can be reduced for higher rotor pole numbers. Generally speaking, a change in pole number always calls for an adaption of the drive geometry.
- The 2-pole rotor shows anisotropic passive stiffness in radial and tilt direction - the 4-pole rotor does not. Depending on the application and the operation frequency, this may demand for higher damping.
- Due to the slotless design, the winding space is directly related to the air gap width. Larger air gaps provide more winding space and allow higher total torque but also decrease the air gap flux density and the torque per ampere rating.
- With larger air gaps, the passive stiffness values (both positive and negative) decline monotonically. The active radial force capacity behaves similar to the torque capacity.
- The analytically estimated iron losses are not significantly different for the 2 rotor types and the original dimensions.
- Only a very limited number of winding schemes produces both, bearing forces and torques, and is practically feasible for motors with geometric dimensions similar to the originally regarded design.

- Other than for the torque, the order of magnitude of the bearing forces can not be directly deduced from the according winding factors.
- A toroid winding form can be an interesting alternative to conventional air gap windings if the winding pitch is high.

Instead of coming up with a clear decision on which rotor pole number is best suited for a bearingless permanent magnet disk drive, the answer depends on the application alone. Possible specifications might e.g. concern maximum tolerable rotor deflections in all degrees of freedom, minimum required torque or advantageous rotordynamic properties, thus demanding certain minimum stiffness and damping values, required winding space and current densities or distinct placement of the resonance frequencies. All of these requirements entail different adaptions of the drive parameters and thus, either one of the two rotor types can be preferable. Nevertheless, the understanding of the variable system parameters and their effects on the overall drive properties are of fundamental importance for a successful design.

6 Acknowledgement

This work was conducted within the strategic research program at the Austrian Center of Competence in Mechatronics (ACCM), which is a part of the COMET K2 program of the Austrian Government. The projects are kindly supported by the Austrian Government, the Upper Austrian Government and the Johannes Kepler University, Linz. The authors thank all involved partners for their support.

References

[1] H. Mitterhofer and W. Amrhein. Design aspects and test results of a high speed bearingless drive. *Proc. 9th Power Electronics and Drive Systems Conference*, 2011.

[2] H. Mitterhofer and W. Amrhein. Motion control strategy and operational behaviour of a high speed bearingless disc drive. In *Proc. IET Power Electronics, Machines and Drives Conference*, 2012.

[3] Ch. Huettner. Nonlinear state control of a left ventricular assist device (lvad). *Proc. International Symposium on Magnetical Bearings*, 2000.

[4] H. Grabner, H. Bremer, W. Amrhein, and S. Silber. Radial vibration analysis of bearingless slice motors. *Proc. 9th International Symposium on Magnetic Bearings*, 2004.

[5] H. Mitterhofer, D. Andessner, and W. Amrhein. Analytical and experimental loss examination of a high speed bearingless drive. In *Proc. International Symposium on Power Electronics Electrical Drives Automation and Motion (SPEEDAM)*, 2012.

[6] S. Silber. Force and torque model for bearingless pm motors. *Proc. International Power Electronics Conference, Tokyo*, 2000.

[7] G. Schweitzer and E. Maslen. *Magnetic Bearings*. Springer, Berlin, 2009.

[8] S. Silber, W. Amrhein, H. Grabner, and R. Lohninger. Design aspects of bearingless torque motors. *Proc. 13th International Symposium on Magnetic Bearings*, 2012.